

# Diffusion Coefficients in Ionic Liquids: Relationship to the Viscosity<sup>†</sup>

Richard Brookes, Alun Davies, Gyanprakash Ketwaroo, and Paul A. Madden\*

Chemistry Department, University of Oxford, South Parks Road, OX1 3QZ, UK

Received: August 12, 2004; In Final Form: October 23, 2004

The relationship between the diffusion coefficient and the viscosity has been examined in computer simulations for a number of ions diffusing in a molten salt (alkali halide) solvent. The comparison gives a measure of a hydrodynamic radius for the diffusing ions which is then compared with the bare ionic radius and a characteristic radius of the coordination complex formed by halide ions around polyvalent cations.  $K^+$  and  $Cl^-$  ions appear to diffuse as isolated spherical particles, whereas the trivalent cations  $Sc^{3+}$ ,  $Y^{3+}$ , and  $La^{3+}$  diffuse as if with an intact coordination shell. These different behaviors can be related to the time scale for the relaxation of the coordination shell, compared to the structural relaxation time of the solvent.

## I. Introduction

A quantitative understanding of the relationship between the diffusion coefficient and the viscosity of a liquid has been one of the long-standing goals of liquid-state research.<sup>1</sup> For ions in ionic liquids, this is a matter of practical as well as fundamental significance. The diffusion coefficient is an important parameter in electrokinetics and, given the importance of molten salts in technologies such as metal extraction<sup>2</sup> or the pyrochemical processing of nuclear waste,<sup>3</sup> it is important to understand how the diffusion coefficient value is affected by changes in the solvent and how it depends on the ionic charge and size. In these technologies, the melt of interest will usually contain the electroactive ion dissolved in a molten salt solvent, such as the low-melting eutectic mixture of LiCl and KCl (46% LiCl), and it is on such solutions of polyvalent ions in alkali halides that we will focus here.

As in all liquids, the state-dependence of the diffusion coefficient follows that of the viscosity

$$D = \frac{kT}{c\pi\eta} \quad (1.1)$$

but there is considerable uncertainty about the value of the coefficient of proportionality,  $c$ , which has the dimensions of a length and is affected by the strength of the interaction of the ion with its surroundings. In molten salts this interaction can be tuned quite finely by varying the identities of the ions over the wide available range, and the viscosity varied extensively. There is a good understanding of the structure of (at least) the first coordination shell from diffraction,<sup>4</sup> spectroscopy,<sup>5</sup> and simulation,<sup>6</sup> so that these materials form an interesting test-bed for the evaluation of ideas about the geometrical significance of the length  $c$ .

In the hydrodynamic limit of a large, massive particle diffusing in a continuous medium, the constant  $c$  is given by the particle radius  $a$  multiplied by 4 or 6, depending on whether slip or stick boundary conditions are imposed at the particle surface ("Stokes' law").<sup>7,8</sup> In simple, unassociated liquids, this relationship is often found to hold for molecular diffusion with a reasonable effective molecular radius when the slip boundary

condition is imposed.<sup>9,10</sup> In aqueous ionic solutions, where there can be a strong interaction between the ion and a coordination shell of water molecules, especially for small or highly charged ions, the relationship can fail qualitatively if  $a$  is taken to be the crystallographic radius of the ion. In some cases, compliance with Stokes' law can be restored by using as the hydrodynamic radius the radius of a "solventberg" of water molecules,<sup>11</sup> which are presumed to be so strongly coordinated to the ion of interest that they are decoupled from the shear relaxation of the solvent.<sup>12,13</sup> There is no theory of this effect, though a number of empirical relationships have been noted; indeed, there is unlikely to be a theory until an understanding of the quantitative success of Stokes' law for *molecular* motion in an unassociated liquid is itself established.<sup>8</sup>

For cations diffusing in molten salts, the situation appears to be very similar to that found in the aqueous solution – Stokes' law with the crystallographic radius does not hold; instead, the hydrodynamic radius of the ion appears to increase with the imagined strength of the interaction of the cation with its coordination shell of anions. It has been observed<sup>14</sup> that the literature data<sup>15,16</sup> on the diffusion coefficients of trivalent metal ions in the Li/KCl eutectic mixture solvent indicates that ions of different radii have very similar diffusion coefficients at a given temperature. Given the importance of these systems (which include most of the lanthanide and actinide ions of interest in nuclear waste reprocessing, inter alia), we have carried out computer simulation investigations of Stokes' relationship for dilute solutions of  $MCl_3$  compounds in the LiCl–KCl mixture for cations with a range of ionic radii. The objectives are to allow the link between local structure and dynamics in this particular system to be investigated and to provide more general insight into the value of the hydrodynamic radius which would be applicable to other classes of partially associated liquid. The molten salts are an attractive testbed for this general goal because they are composed of *spherical* particles with well-defined sizes, in contrast to molecular liquids. Experimentally, it is difficult to measure the diffusion coefficient accurately because of the inconvenience of dealing with high-temperature corrosive liquids; we circumvent this problem by using viscosities and diffusion coefficients from computer simulations. Similar studies of the undoped LiCl–KCl system<sup>17</sup> have already shown that Stokes' law behavior is found to hold with

<sup>†</sup> Part of the special issue "David Chandler Festschrift".

\* Corresponding author. E-mail: paul.madden@chemistry.oxford.ac.uk.

**TABLE 1: Ionic Diffusion Coefficients ( $D_\alpha/10^{-5} \text{ cm}^2 \text{ s}^{-1}$ ) in the Dilute Solutions of  $\text{MCl}_3$  in the  $\text{LiCl/KCl}$  Mixture at 1096 K<sup>a</sup>**

	Sc	Y	La	nondoped
$\text{Cl}^-$	7.72	7.47	7.65	7.98
$\text{Li}^+$	9.34	8.95	8.90	8.04
$\text{K}^+$	8.82	8.02	8.07	8.19
$\text{M}^{3+}$	3.14	2.77	2.95	

<sup>a</sup> Note that  $D_{\text{Li}} = 17.3 \times 10^{-5} \text{ cm}^2 \text{ s}^{-1}$  and  $D_{\text{Cl}} = 9.51 \times 10^{-5} \text{ cm}^2 \text{ s}^{-1}$  in pure  $\text{LiCl}$  at 1100 K.<sup>22</sup>

hydrodynamic radii close to the crystal radii of the ions, though there is some composition dependence.

Here, dilute mixtures of 2%  $\text{MCl}_3$  in an equimolar  $\text{LiCl-KCl}$  mixture have been simulated with interactions described by Born–Mayer ionic pair potentials supplemented with anion polarization effects. Extensive investigations of the structure of pure  $\text{MCl}_3$  melts with these potentials have already been carried out.<sup>6,18,19</sup> The details of the calculations are described in appendix.

## II. Diffusion Coefficients and Viscosities

Solutions of  $\text{ScCl}_3$  (crystal radius<sup>20</sup>  $r_{\text{Sc}} = 0.81 \text{ \AA}$ ),  $\text{YCl}_3$  ( $r_{\text{Y}} = 0.93 \text{ \AA}$ ), and  $\text{LaCl}_3$  ( $r_{\text{La}} = 1.15 \text{ \AA}$ ) in the  $\text{LiCl-KCl}$  mixture have been simulated at 1096 K, and the ionic diffusion coefficients calculated according to the Einstein relationship

$$D_\alpha = \lim_{t \rightarrow \infty} \frac{1}{6t} \langle |\vec{r}_{i\alpha}(t) - \vec{r}_{i\alpha}(0)|^2 \rangle \quad (2.1)$$

where  $\vec{r}_{i\alpha}$  is the position of ion  $i$  of species  $\alpha$ . These are shown in Table 1 together with the calculated and experimental values for the  $\text{Li}^+$ ,  $\text{K}^+$ , and  $\text{Cl}^-$  ions of the undoped mixture.<sup>17,21</sup> We can see that the introduction of the low concentration of dopant cations has little effect on the diffusion of the “solvent” ions, and furthermore that the diffusion coefficients of the  $\text{M}^{3+}$  ions are 3 to 4 times smaller than those of the monovalent species. The diffusion coefficients for all three trivalent cations are very similar.

Further simulations of the  $\text{YCl}_3$  and  $\text{LaCl}_3$  systems across a wide range of temperatures, but the same density as the 1096 K runs, shows close agreement between calculated diffusion coefficients for  $\text{Y}^{3+}$  and  $\text{La}^{3+}$  despite the differences in their crystallographic radii, as is evident from Figure 2. The figure also shows experimental data for  $\text{U}^{3+}$  in the  $\text{Li/KCl}$  eutectic;  $\text{U}^{3+}$  has a very similar size to  $\text{La}^{3+}$  ( $r_{\text{U}^{3+}} = 1.16 \text{ \AA}$ ), and its diffusion coefficient agrees with that calculated at the higher temperatures where, as we shall see, the viscosity of the simulated fluid is close to that of the real eutectic mixture.

The shear viscosities are calculated from the time integral of the autocorrelation function of the anisotropic elements of the stress tensor, i.e.,

$$\eta = \lim_{t \rightarrow \infty} \eta(t) \quad (2.2)$$

where

$$\eta(t) = \frac{1}{kTV} \int_0^t \langle \sigma_0^{\alpha\beta}(0) \sigma_0^{\alpha\beta}(\tau) \rangle d\tau \quad (2.3)$$

Here,  $\sigma^{\alpha\beta}$  could be any of the five independent anisotropic components of the stress tensor, such as  $\sigma^{\text{xy}}$ , and we may average over these five quantities in order to improve the statistics. Figure 3 shows the time evolution of the five stress tensor correlation functions for the  $\text{LaCl}_3$  in  $\text{LiCl-KCl}$  system.

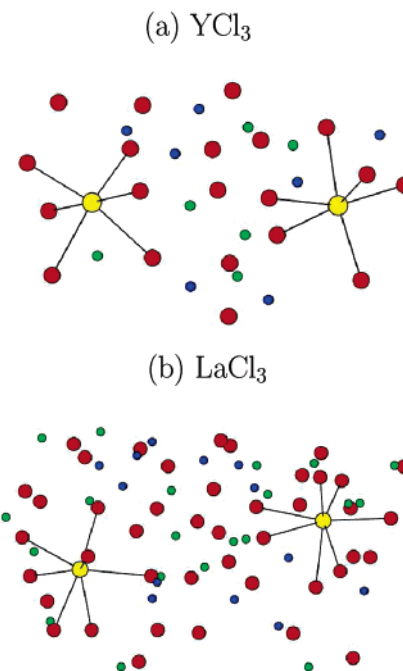


**Figure 1.** Molecular graphics snapshots of the local coordination environments around (a)  $\text{Y}^{3+}$  and (b)  $\text{La}^{3+}$  in the  $\text{LiCl-KCl}$  mixture at 1096 K.  $\text{M}^{3+}$  ions are yellow,  $\text{Cl}^-$  red,  $\text{Li}^+$  green, and  $\text{K}^+$  blue.

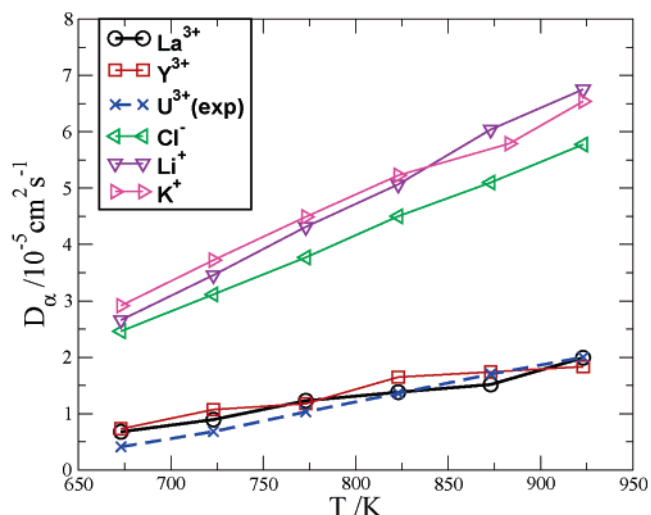


**Figure 2.** Temperature dependence of the ionic diffusion coefficients for  $\text{YCl}_3$  and  $\text{LaCl}_3$  in the  $\text{LiCl-KCl}$  mixture. Experimental data is shown<sup>15</sup> for  $\text{U}^{3+}$  (crystal radius  $r_{\text{U}} = 1.16 \text{ \AA}$ , very similar to that of  $\text{La}^{3+}$ ). The values given for the monovalent species are the mean values from the two mixtures.

Although the individual functions are quite noisy (even after  $\sim 2$  million MD steps) they oscillate about a common value and their average is reasonably smooth. We can see that the running integral of this averaged function reaches a plateau value after about 3 ps, and the viscosity is calculated from it. Three picoseconds represents the time scale of the structural relaxation of the system. The calculated viscosities of the  $\text{ScCl}_3$ ,  $\text{YCl}_3$ , and  $\text{LaCl}_3$  mixtures are very similar at 0.87, 0.87, and 0.88  $\text{mNsm}^{-2}$ ; at 1096 K these values are 5% lower than reported for the simulation of the undoped eutectic mixture (at a slightly higher density).<sup>17</sup> Again, the addition of the dopant species appears to have very little effect on the bulk properties of the solvent. The values are in excellent agreement with the experimental value of 0.88  $\text{mNsm}^{-2}$  at 1096 K,<sup>21</sup> but for lower

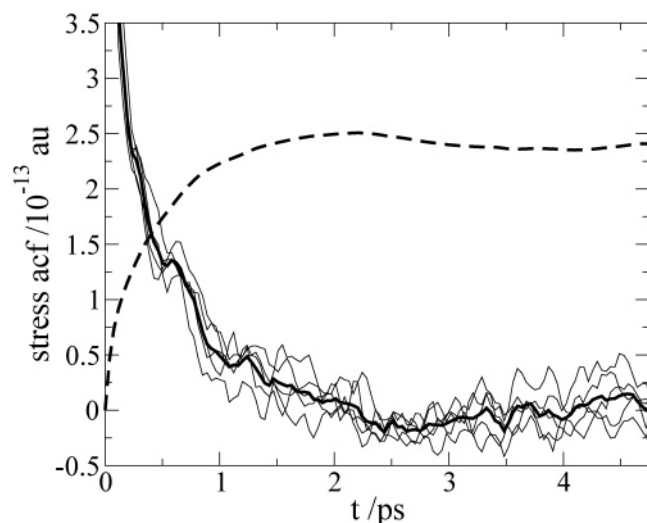


**Figure 3.** Time evolution of the stress tensor correlation function in the  $\text{LaCl}_3$  in  $\text{LiCl-KCl}$  system at 723 K. The integral, from which the viscosity is calculated, reaches a plateau value after about 3 ps, which represents the time scale for structural relaxation.

**TABLE 2: Calculated Hydrodynamic Radii (in Å) for the Ions in the Dilute Solutions of  $\text{MCl}_3$  in the  $\text{LiCl/KCl}$  Mixture at 1096 K**

radius	$\text{Cl}^-$	$\text{K}^+$	$\text{Li}^+$	$\text{Sc}^{3+}$	$\text{Y}^{3+}$	$\text{La}^{3+}$
slip	1.81	1.66	1.52	4.41	5.11	4.98
stick	1.21	1.10	1.01	2.94	3.411	3.32
Shannon	1.67	1.52	0.73	0.89	1.04	1.18

temperatures the calculated viscosities drop below the experimental values, probably because the density has been kept constant.

Stokes' law, eq 1.1, can be rearranged to give an expression for the hydrodynamic radius of an ion in terms of the its diffusion coefficient and the viscosity,

$$a_\alpha = \frac{kT}{c'\pi\eta D_\alpha} \quad (2.4)$$

where  $c'$  is 4 or 6 depending upon slip or stick boundary conditions. At the atomistic level, two assumptions can be made about the nature of the interaction of the diffusing particle with surrounding solvent particles, which translates into different boundary conditions. A spherical diffusing particle will exert a purely radial force on its neighbors, and this may be shown to result in slip behavior when integrated up to the hydrodynamic limit.<sup>23</sup> On the other hand, a structured diffusing particle, which allows some interdigitation of solvent particles into the crevices on its surface, will exert an additional tangential acceleration of the surrounding fluid, and this leads to stick behavior.

Values of the hydrodynamic radii calculated from eq 2.4 with the slip and stick boundary conditions are given in Table 2 and are compared with the Shannon crystal radii for the appropriate coordination numbers.<sup>20</sup> We have used the calculated viscosities and diffusion coefficients to obtain these values, so that the measure is derived entirely from the properties of the simulated fluid. For the  $\text{La}^{3+}$  and  $\text{Y}^{3+}$  solutions these were available at seven temperatures from 650 to 1096 K (as illustrated in Figure 2). There was no systematic change of the hydrodynamic radius with temperature, and the values given in the table for all the ions except  $\text{Sc}^{3+}$  are averages over these different runs. We simulated the  $\text{Sc}^{3+}$  only at 1096 K, and, consequently, the value given for this ion is less well-averaged than for the other cases.

It can be seen that for the larger, singly charged  $\text{K}^+$  and  $\text{Cl}^-$  ions, which can be anticipated to be most weakly coordinated to their surroundings, the radii calculated from the slip boundary conditions are in good agreement with their crystal radii. These appear, from this perspective, to be diffusing as single, spherical ions (slip boundary conditions). For the remaining ions, however, the hydrodynamic radii are significantly larger than the bare crystal radii.

For these other cases, we can examine the idea that the ions are diffusing with an intact coordination shell which behaves as if rigidly attached to the central cation. Figure 1 shows molecular graphics snapshots of  $\text{YCl}_3$  and  $\text{LaCl}_3$  in the  $\text{LiCl-KCl}$  mixture at 1096 K. "Bonds" are drawn between  $\text{M}^{3+}$  ions and  $\text{Cl}^-$  ions if their separation is less than the position of the first minimum in the relevant  $\text{M-Cl}$  partial radial distribution function, and the existence of coordination polyhedra can clearly be seen. In the  $\text{YCl}_3$  case, there are two  $\text{YCl}_6^{3-}$  octahedra, and in the  $\text{LaCl}_3$  case there are two  $\text{La}^{3+}$  ions that are 7-coordinated to  $\text{Cl}^-$  ions at this instant. The existence of these coordination complexes in the molten salt solutions is well-established from Raman spectroscopy,<sup>5</sup> though the time scales on which they exist and the way in which they affect transport properties are not known. They give rise to discrete vibrational bands in the  $100\text{ cm}^{-1}$  to  $350\text{ cm}^{-1}$  range, so they are certainly stiff compared to the surrounding fluid, if not really rigid. Such Raman spectra have been reproduced in simulations with the same potentials as used here.<sup>24,25</sup>

In Figure 4 we illustrate the relationship between the hydrodynamic radius calculated from the *stick* boundary condition for  $\text{Sc}^{3+}$ ,  $\text{Y}^{3+}$ , and  $\text{La}^{3+}$  and various structural features of the coordination shell. The stick boundary condition seems more appropriate in these cases because the coordination complex has a structured surface, and allows for interdigitation of the alkali cations.<sup>25</sup> The full line is the  $\text{M}^{3+}-\text{Cl}^-$  radial distribution function,  $g_{\text{MCl}}(r)$  and the dotted line is its running integral,

$$n_{\text{MCl}}(R) = 4\pi\rho_{\text{Cl}^-} \int_0^R dr r^2 g_{\text{MCl}}(r) \quad (2.5)$$

where  $\rho_{\text{Cl}^-}$  is the number density of chloride ions, which gives the running value for the coordination number of  $\text{Cl}^-$  ions around the cation. The position of the hydrodynamic radius is indicated by the vertical dashed line. It can be seen to lie well outside the first peak of  $g_{\text{MCl}}(r)$  in all three cases.

The choice of a particle size to reflect the radius of a diffusing coordination complex in a hydrodynamic model is somewhat subjective, but we suggest that a good choice would be the distance to which the surrounding fluid approaches the central cation and estimate this from the position of the first peak of the  $\text{M}^{3+}$  alkali cation radial distribution function *minus* the crystal radius of the alkali cation. This distance is indicated by the dashed-dot vertical line in the figure. The hydrodynamic radii obtained from the simulated diffusion coefficients and viscosities are seen to be in good agreement with this estimate. For  $\text{Y}^{3+}$  the agreement is excellent; for  $\text{La}^{3+}$  and  $\text{Sc}^{3+}$  the hydrodynamic radius is slightly smaller than the model value, which indicates (at the risk of over-interpreting the data) that  $\text{Y}^{3+}$  diffuses as if with a rigid coordination shell, whereas, for  $\text{La}^{3+}$  and  $\text{Sc}^{3+}$  there is some relaxation of the coordination shell in the process of diffusion. We will explore this idea further below.

The final (bottom-right) panel of Figure 4 shows a similar comparison for the remaining case of  $\text{Li}^+$ . Here the hydrodynamic radius obtained from the *slip* boundary condition (vertical

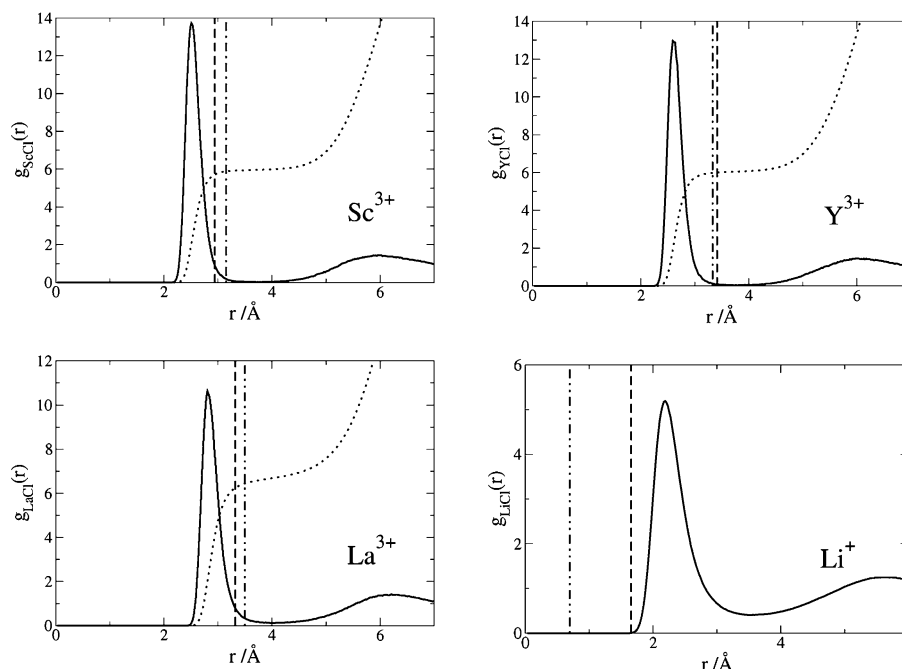


**Figure 4.** M–Cl partial radial distribution function (full) and its running integral (dots) are compared with the hydrodynamic radii  $a_{sc}$  (vertical dashed line). Also shown, in the panels for the  $M^{3+}$  ions, is a measure of the size of the coordination complex (dash–dot): in the  $Li^+$  case this line represents the bare ion size.

dashed line) is compared with  $g_{LiCl}$ . As with the other monovalent ions, it can be seen to lie well inside the first peak of  $g_{LiCl}$  but, unlike the  $K^+$  and  $Cl^-$  cases, it is still considerably larger than the crystal radius of the  $Li^+$  ion (or, equivalently, the maximum of  $g_{LiCl}$  minus the  $Cl^-$  crystal radius), as shown by the dashed–dot line.  $Li^+$  is therefore behaving in an intermediate manner between the bare ion diffusion exhibited by  $Cl^-$  and  $K^+$  and the (almost) intact coordination shell of the  $M^{3+}$  ions, and rather closer to the former – as if its coordination shell undergoes substantial relaxation.

### III. Relaxation of the $M^{3+}$ Coordination Shell

We now try to identify a more direct measure of the properties of the coordination shell which will enable us to rationalize why, from the Stokes' law perspective, the  $M^{3+}$  ions appear to diffuse with an intact shell, in contrast to the monovalent ions, and the intermediate status of the  $Li^+$  ion. Previous work on ions in aqueous solutions has suggested that some characteristic relaxation time of the coordination shell should be compared with a structural relaxation time of the solvent.<sup>12,13</sup>

The rate of the break-up of the coordination polyhedra can be investigated using the cage correlation function analysis introduced by Rabani et al.<sup>26,27</sup> The instantaneous set of neighboring ions of any given ion,  $i$ , of species  $\alpha$ , is defined by a neighbor list,  $\vec{l}_i(t)$ , which gives the identities of those ions of the other species,  $\beta$ , which lie within the first coordination shell of ion  $i$ , defined by the position,  $r_{\alpha\beta}^{\min}$ , of the first minimum in the partial radial distribution function  $g_{\alpha\beta}$ .  $\vec{l}_i(t)$  is a vector of dimension  $N_\beta$ , with a 1 entered for any counterion within the coordination shell of  $i$ , and a 0 otherwise. Hence,  $|\vec{l}_i(t)|^2$  gives the number of counterions in the coordination shell of  $i$  at time  $t$ , and the number of ions that have left ion  $i$ 's original neighbor list in the subsequent time interval  $\delta t$  is

$$n_i^{\text{out}}(t, t + \delta t) = |\vec{l}_i(t)|^2 - \vec{l}_i(t) \cdot \vec{l}_i(t + \delta t) \quad (3.1)$$

**TABLE 3: Cage Decay Rates and Cage Lifetime of the Cation–Anion Cages in Dilute Solutions of  $MCl_3$  in the LiCl/KCl Mixture at 1096 K**

	$K^+$	$Li^+$	$Sc^{3+}$	$Y^{3+}$	$La^{3+}$
$\tau/10^{-12}s$	0.19	0.51	16.0	10.0	2.4

The cage correlation function for the cage decay is then

$$C_{\text{cage}}^{\text{out}}(t) = \left\langle \frac{1}{N_\alpha} \sum_{i \in \alpha} \Theta(c - n_i^{\text{out}}(0, t)) \right\rangle \quad (3.2)$$

where  $c$  is the number of counterions that must enter or leave an ion's neighbor list before the coordination cage is considered to have decayed, and  $\Theta$  takes the value 1 if its argument is greater than zero, and the value 0 otherwise. In this work  $c = 1$ , and the cage correlation function measures the rate at which a single counterion *leaves* the cage. We can define the time,  $\tau$ , for the cage correlation function to fall to a value of  $1/e$  as the *cage lifetime*. On this time scale,  $(1/e)$ th of the cations in the system will have lost one of the counterions from their coordination shell.

The cage lifetimes for the  $M^{3+}$  cations are shown in Table 3. The lifetimes of these cages are much longer than those of the relatively weakly coordinated solvent cations,  $Li^+$  and  $K^+$ . Furthermore, we can see that the lifetime of the  $La^{3+}$  coordination complex is considerably shorter than those for  $Sc^{3+}$  and  $Y^{3+}$ . Note from the running integral in Figure 4 that  $Y^{3+}$  and  $Sc^{3+}$  have a coordination number very close to six in this mixture, whereas for the larger  $La^{3+}$  the coordination number is slightly larger, closer to seven. The cage decay rate suggests that this outermost ion is relatively labile in  $La^{3+}$ . Despite this, the hydrodynamic radius shows that coordination shell appears to persist for sufficiently long to diffuse in a nearly rigid manner.

The critical time scale to which the cage relaxation time should be compared is set by the structural relaxation time of the solution, i.e., the time scale on which the fluid relaxes after an imposed shear. If the coordination complex is "rigid" on this time scale it does not participate in the shear relaxation.



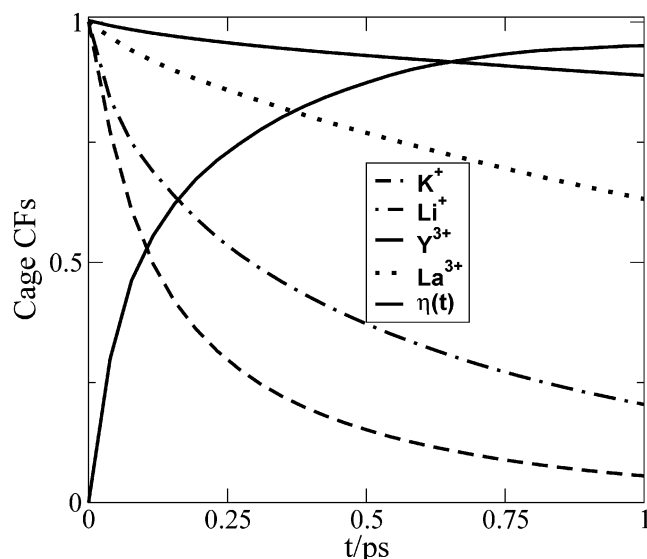


**Figure 5.** Cation–anion cage correlation functions for  $Y^{3+}$ ,  $La^{3+}$ ,  $Li^+$ , and  $K^+$  in the  $LiCl$ – $KCl$  mixtures at 1096 K are compared with the running integrals of the mean stress tensor correlation function (shown on an arbitrary vertical scale), i.e., the quantity  $\eta(t)$  from eq 2.3 and Figure 3.

**TABLE 4: Born–Mayer Parameters for the  $MCl_3$  Systems (all values in atomic units)**

Ion pair	$a_{ij}$	$B_{ij}$	$C_6$	$C_8$	$b_6$	$b_8$
Sc–Sc	2.798	20.0	15.0	20.0	1.90	1.80
Sc–Cl	1.80	195.0	15.2	100.0	1.50	1.51
Y–Y	2.798	20.0	15.0	200.0	1.90	1.80
Y–Cl	1.80	263.0	45.2	1000.0	1.50	1.51
La–Cl	1.80	450.2	102.2	0.0	1.50	1.51
La–La	2.798	20.0	15.0	200.0	1.90	1.80
K–K	1.5616	54.4930	25.3822	89.5215	—	—
K–Li	1.5690	10.5448	1.3892	3.1668	—	—
K–Cl	1.5479	57.7257	50.1377	272.2945	—	—
Li–Li	1.5717	1.9748	0.0761	0.1119	—	—
Li–Cl	1.5563	12.4231	2.0891	8.9521	—	—
Cl–Cl	1.5717	71.3445	130.0445	932.5154	—	—

Figure 5 shows the running integral of the stress tensor correlation function (as in Figure 3) compared with the cation–anion cage correlation functions. We can see that the decay of the  $K^+$  cage is complete (or almost so) on the time scale of the structural relaxation of the system, as defined by the emergence of the plateau in the integrated stress tensor correlation function, and hence that this cage has only a transient existence and can contribute fully to the relaxation of a shear imposed upon the fluid. This behavior seems consistent with the observation that the hydrodynamic size of a  $K^+$  ion is the bare crystal radius. The same is also true for the cage of cations around a  $Cl^-$  ion, for which the cage correlation function is almost indistinguishable from that of  $K^+$ . The  $M^{3+}$  coordination polyhedra are much longer lived. For  $Y^{3+}$  the cage remains intact on the time scale of structural relaxation, and even for  $La^{3+}$  this is almost the case. It is tempting to associate this difference with the observation that the hydrodynamic radius for  $La^{3+}$  is smaller than that suggested by the geometrical model, as if a smaller fraction of the coordination complex was rigid in the  $La^{3+}$  case, whereas close agreement is found for  $Y^{3+}$ .<sup>28</sup> The relaxation of the  $Li^+$  cage appears to occur on the same time scale as that of the stress tensor, which is consistent with the intermediate value of the hydrodynamic radius – between that of the bare ion and the coordination complex and closer to the former than the latter.

**TABLE 5: The Dipole Damping Parameters in the  $MCl_3$  Systems (all values in atomic units)<sup>a</sup>**

ion pair	$b$	$c$
Sc–Cl	1.336	1.0
Y–Cl	1.336	1.0
La–Cl	1.258	1.0
Li–Cl	1.72	2.0
K–Cl	1.46	2.8

<sup>a</sup> The chloride dipole polarizability is 19.145 au.

#### IV. Closing Remarks

The original motivation for this study was to explain the observation that the diffusion coefficients of a range of trivalent cations in the  $Li/KCl$  eutectic mixture was almost independent of cation size.<sup>14</sup> It turns out that these molten salt mixtures are an attractive testing ground for ideas about the relationship between the diffusion coefficient and viscosity, presenting systems that can be simulated realistically and to which simple geometrical ideas about coordination structures are readily applied. We have distinguished two intuitively appealing ideal behaviors in the hydrodynamic radius: diffusion as a monovalent ion with “slip” boundary conditions (shown by  $K^+$  and  $Cl^-$ ) and diffusion as an intact coordination complex exhibiting stick boundary conditions ( $Sc^{3+}$ ,  $Y^{3+}$  and  $La^{3+}$ ), with  $Li^+$  emerging as an intermediate case. These different behaviors can be linked to the time scale of relaxation of the coordination shell compared to the structural relaxation time of the solvent. The best geometrical radius to associate with the coordination complex around a cation appears to be the distance at which the surfaces of the alkali cations from the solvent are first encountered. Because this distance is  $\sim$  (cation – radius +  $A$ ), where  $A$  is a (constant) coordination shell thickness which is at least twice as big as the cation radius itself, the diffusion coefficients for related cations are insensitive to the bare cation radii.

**Acknowledgment.** This work was supported by EPSRC grant GR/R57584/01. It was begun when P.A.M. was visiting JAERI (Tokaimura) as a guest of T. Ogawa and Y. Okamoto.

#### Appendix: Details of the Simulations

All of the systems have been simulated using a simple Born–Mayer potential,

$$U_{ij}(r_{ij}) = \frac{Q_i Q_j}{r_{ij}} + B_{ij} e^{-\alpha_{ij} r_{ij}} - \sum_{n=6,8} \frac{C_{ij}^n}{f_{ij}^n r_{ij}^n} \quad (A.1)$$

to represent short-range repulsion, charge–charge, and dispersion interactions between the ion pairs together with an account of the (many-body) induction forces arising from the anion dipole polarization.<sup>29</sup> In eq A.1,  $Q_i$  is the ionic charge (taken as the formal valence in the models), the exponential represents short-range repulsion, and the terms in  $r^{-n}$  represent dispersion interactions. In the latter,  $f_n$  is a Tang–Toennies<sup>30</sup> damping function, which is applied between unlike-charged ions, and whose range is given by the parameter  $b_n$ . The potential parameters are given in Table 4, and are based on original potentials given in refs 31 and 32 and developed in ref 6. The remaining unlike cation–cation potentials were assumed to be identical, because the cations, with their like charges, will seek to repel each other, and so the exact form of the potential will have very little effect on the properties of the simulated fluid. The  $Li$ – $K$  potential was therefore arbitrarily used for these other cation–cation potentials.

The parameters controlling the dipole induction are as given in Table 5, as obtained from electronic structure calculations,<sup>33</sup> and have the meanings explained in that paper.

The simulations were performed at the experimental density for the undoped system at 1096 K, and statistics were recorded for runs of length  $1-3 \times 10^6$  time steps, necessary to get reproducible values for the viscosity, with a time step of 8au, required to integrate the fast dipole motion using a Car–Parrinello-type algorithm.<sup>29</sup> The systems contained 102 Cl<sup>−</sup> ions, 51 Li<sup>+</sup> ions, 51 K<sup>+</sup> ions, and 2 M<sup>3+</sup> ions. Ewald summations were used for all charge and dipole interactions.

## References and Notes

- (1) Chandler, D. *J. Chem. Phys.* **1975**, *62*, 1358.
- (2) Grjotheim, K.; Krohn, C.; Malinovsky, M.; Matiasovsky, K.; Thonstad, J. *Aluminium Electrolysis, Fundamentals of the Hall–Heroult Process*; Springer-Verlag: Dusseldorf 1982.
- (3) Matsuura, H.; Takagi, R.; Zbalocka-Malicka, M.; Rycerz, L.; Szczepaniak, J. *J. Nucl. Sci. Technol.* **1997**, *33*, 895.
- (4) Wasse, J. C.; Salmon, P. S. *J. Phys.: Condens. Matter* **1999**, *11*, 645.
- (5) Photiadis, G. M.; Borreson, B.; Papatheodorou, G. N. *J. Chem. Soc., Faraday Trans.* **1997**, *94*, 2605.
- (6) Hutchinson, F.; Madden, P. A.; Wilson, M. *Mol. Phys.* **2001**, *99*, 811.
- (7) Landau, L. D.; Lifshitz, E. M. *Fluid Mechanics*; Pergamon Press: Oxford, 1963.
- (8) Masters, A. J.; Madden, P. A. *J. Chem. Phys.* **1981**, *74*, 2450.
- (9) Jonas, J. *J. Chem. Phys.* **1976**, *65*, 582.
- (10) Stokes' law is not always followed in such fluids. It breaks down in strongly supercooled liquids and in mixtures where the mass and size ratios between solute and solvent are large. Such effects were examined in Nuevo, M. J.; Morales, J. J.; Heyes, D. M. *Mol. Phys.* **1997**, *91*, 769, inter alia.
- (11) Bockris, J. O'M.; Reddy, A. K. N. *Modern Electrochemistry*; Butterworths: London, 1955.
- (12) Wolynes, P. G. *Annu. Rev. Phys. Chem.* **1980**, *31*, 345.
- (13) Impey, R. W.; McDonald, I. R.; Madden, P. A. *J. Phys. Chem.* **1983**, *87*, 5071.
- (14) Private communication from Toru Ogawa (JAERI).
- (15) Martinot, L.; Calligary, F. *Atomic Energy Rev.* **1973**, *11*, 23.
- (16) Martinot, L.; Reul, J.; Duyckaerts, G.; Mueller, W. *Anal. Chem.* **1975**, *28*, 233.
- (17) Iizuka, M. *J. Electrochem. Soc.* **1998**, *145*, 84.
- (18) Morgan, B.; Madden, P. A. *J. Chem. Phys.* **2003**, *119*, 7471.
- (19) Hutchinson, F.; Rowley, A. J.; Walters, M. K.; Wilson, M.; Madden, P. A.; Wasse, J. C.; Salmon, P. S. *J. Chem. Phys.* **1999**, *111*, 2028.
- (20) Hutchinson, F.; Wilson, M.; Madden, P. A. *J. Phys.: Condens. Matter* **2000**, *12*, 10389.
- (21) Shannon crystal radii from <http://www.webelements.com/>.
- (22) Janz, G. J. *J. Phys. Chem. Ref. Data* **1998**, *17*, suppl. 2. Janz, G. J. *J. Phys. Chem. Ref. Data* **1982**, *10*, 505.
- (23) Lenke, R.; Uebelhack, W.; Klemm, A. *Z. Naturforsch. Teil. A* **1973**, *28*, 881.
- (24) Masters, A. J.; Keyes, T. F.; Madden, P. A. *J. Chem. Phys.* **1981**, *75*, 485.
- (25) Madden, P. A.; Wilson, M.; Hutchinson, F. *J. Chem. Phys.* **2004**, *120*, 6609.
- (26) Glover, W. J.; Madden, P. A. *J. Chem. Phys.* **2004**, *121*, 7293.
- (27) Rabani, E.; Gezelter, J. D.; Berne, B. J. *J. Chem. Phys.* **1997**, *107*, 6867.
- (28) Rabani, E.; Gezelter, J. D.; Berne, B. J. *Phys. Rev. Lett.* **1999**, *82*, 3649.
- (29) But we must then account for the fact that Sc<sup>3+</sup> also has a smaller than the geometric radius, whilst this ion has the longest cage relaxation time. This contrary result could be a consequence of the relatively poor statistics for the Sc<sup>3+</sup> case.
- (30) Wilson, M.; Costa Cabral, B. J.; Madden, P. A. *J. Phys. Chem.* **1996**, *100*, 1227.
- (31) Tang, K. T.; Toennies, J. P. *J. Chem. Phys.* **1984**, *80*, 3726.
- (32) Lantelme, F.; Turq, P. *J. Chem. Phys.* **1982**, *77*, 3177.
- (33) Sangster, M. J. L.; Dixon, M. *Adv. Phys.* **1976**, *25*, 247.
- (34) Domene, C.; Fowler, P. W.; Wilson, M.; Madden, P. A. *Mol. Phys.* **2002**, *100*, 3847 and loc. cit.